Theoretical Physics. Quantum Field Theory

UDC 530.182 https://www.doi.org/10.33910/2687-153X-2021-2-3-122-131

Spontaneous symmetry breaking and superposition of states in systems with dynamic chaos

A. V. Liaptsev✉[1]

[1] Herzen State Pedagogical University of Russia, 48 Moika Emb., Saint Petersburg 191186, Russia

Author

Alexander V. Liaptsev, ORCID: 0000-0002-8702-9062, e-mail: upm_eno@mail.ru

For citation: Liaptsev, A. V. (2021) Spontaneous symmetry breaking and superposition of states in systems with dynamic chaos. *Physics of Complex Systems*, 2 (3), 122–131. https://www.doi.org/10.33910/2687-153X-2021-2-3-122-131

Received 2 May 2021; reviewed 26 May 2021; accepted 26 May 2021.

Funding: The study did not receive any external funding.

Abstract. The article discusses one of the typical problems described by the equations of nonlinear dynamics—forced oscillations in a system with *W*-potential. It focuses, in particular, on chaotic oscillations in the presence of dissipation. In this case the state of the system is described by a chaotic (strange) attractor and can be characterized by the probability density in the phase space. A partial differential equation for the probability density is presented. It is shown that when the parameters change in the system under consideration, symmetry breaking can occur. In this case the superposition principle for the probability density is valid. It is similar to the superposition principle for the quantum mechanical function in the problem of particle motion in the *W*-potential field.

Keywords: nonlinear dynamics, strange attractor, probability density, chaos, perturbation theory, superposition principle.

Introduction

The phenomenon of spontaneous symmetry breaking is widespread in various physical systems, from the simplest mechanical systems to objects studied by cosmology. The essence of the phenomenon is that, despite the invariance of the equations of motion describing the system with respect to some transformations of symmetry, the system turns out to be in a state that is not invariant with respect to these transformations. For example, in the theory of molecular spectra, the Hamiltonian of a molecule is invariant under the operations of permutation of identical nuclei and inversion. The corresponding transformations form a complete permutation-inversion group of the nuclei of the molecule (Bunker 1979). However, in real molecules, some of the corresponding movements (permutation of the nuclei, or the movement leading to the inversion of the nuclei) are unrealizable. As a result, the actual symmetry of the molecule is lower than that of the original Hamiltonian. The symmetry group corresponding to the realized motion is defined by the Banker as the molecular symmetry group, which is a subgroup of the symmetry group of the original Hamiltonian.

A typical example is the tetratomic molecules AB_3, whose equilibrium structure of the nuclei is a tetrahedron with the base of a regular triangle (Fig. 1).

The combination of operations of inversion of nuclei and permutation of two identical nuclei results in the new configuration of the molecule, equivalent to the movement of the nucleus *A* through the plane formed by the nuclei *B*. This movement is realized in the NH_3 molecule, but it is not realized in the NF_3 molecule. As a result, the molecular symmetry group of the NH_3 molecule is isomorphic to the point symmetry group $\mathbf{D_{3h}}$, and the molecular symmetry group of the NF_3 molecule is isomorphic to the point symmetry group $\mathbf{C_{3v}}$ (Bunker 1979). Thus, one can say that in the NF_3 molecule the symmetry is broken, unlike in the NH_3 molecule.

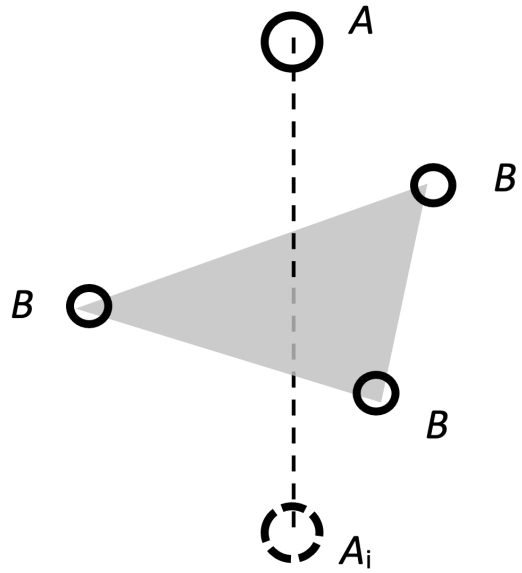

Fig. 1. Tunneling in a molecule AB_3

It should be noted, however, that if the NH_3 molecule is in the lowest vibrational states, then the motion considered above is low probable. In this case, we can talk about tunneling through the potential barrier when the nucleus *A* passes through the plane formed by the nuclei *B*. Taking into account the fact that the motion of the nuclei of a molecule can be considered in a quasi-classical approximation, the description of such tunneling is included in a number of textbooks as an educational task (Landau, Lifshitz 1977). The consequence of tunneling is the splitting of the energy level corresponding to the movement within a single minimum of energy (Fig. 2).

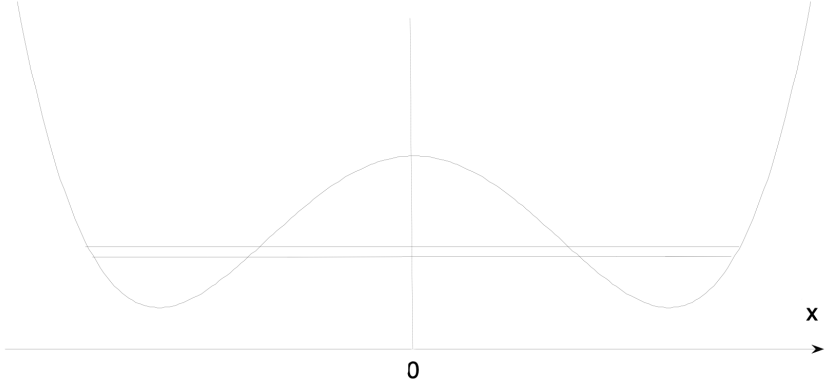

Fig. 2. Splitting in a system with *W*-potential due to tunneling

If we denote the wave function describing the motion in the region of one of the minima in disregard of tunneling through $\psi(x)$, then the wave functions corresponding to the split levels are superposition of the functions describing the motion in each of the corresponding pits:

$$\psi_{\pm}(x) = \frac{1}{\sqrt{2}}\left(\psi(x) \pm \psi(-x)\right).$$

The splitting of the energy levels ΔE is proportional to the tunneling probability. With a low probability, and, accordingly, a small splitting, the probability of detecting a molecule in the region of one of the local minima oscillates according to the law:

$$w = (\sin \Delta E t / \hbar)^2.$$

Since the oscillation period gradually increases with a decrease in the probability of tunneling, it is strictly impossible to determine at what specific value of ΔE the symmetry breaking occurred. In accordance with the definition of Bunker (Bunker 1979), we can assume that the symmetry is broken if the molecule remains in one of the configurations near the local minimum during the observation period. That is, the symmetry is broken at $\Delta E \lesssim t_{obs}/\hbar$, where t_{obs} is the observation time.

Chaotic motion in classical systems with W-potential

The potential shown in Fig. 2, usually called *W*-potential, can be modeled, in particular, by the expression:

$$U(x) = \frac{\alpha x^2}{2} + \frac{\beta x^4}{4},$$

where the parameters $\alpha < 0$ and $\beta > 0$. In classical mechanics, the motion of a body of a unit mass in such a potential in the presence of a viscous friction force and an external periodic force is described by the Duffing equation:

$$\ddot{x} = -\alpha x - \beta x^3 - \gamma \dot{x} + f \sin \omega t. \quad (1)$$

In this equation, the parameter γ characterizes the dissipation, and the parameters f and ω the amplitude and frequency of the external force.

Depending on the parameters of the problem, forced oscillations can capture the regions of both minima, or occur near one of the minima. At a sufficiently large value of the driving force f and a small depth of the pit $\Delta U = \frac{\alpha^2}{4\beta}$, the oscillation captures the regions of both minima, and with a decrease in f and (or) an increase in ΔU, it shifts to the region of one of the pits, without crossing the potential barrier.

A characteristic feature of the solutions of the Duffing equation is the occurrence of chaotic oscillations for certain sets of equation parameters. In the case of chaotic oscillations, the motion extends to both minima. In this case, the chaotic attractor has a certain symmetry, which is well shown in the fractal picture of the Poincare section (Liaptsev 2013). At the same time, with other sets of parameters, the movement can have a regular character, that is, be periodic. The system described by the Duffing equation with the parameter $\gamma > 0$ is a typical example of a dissipative system in which chaotic motion has certain features. Equation (1) can be written as an autonomous system of three differential equations of the 1st order:

$$\begin{aligned} \dot{x} &= v \\ \dot{v} &= -\alpha x - \beta x^2 - \gamma v + f \sin\varphi \\ \dot{\varphi} &= \omega \end{aligned} \quad (2)$$

The trajectory of the system in chaotic motion tends to the chaotic attractor (strange attractor). Since the dependence of the right side of equations (2) on the variable φ is determined by the periodic function, we can assume that $\varphi \in [0, 2\pi]$. The trajectory of motion in the phase space can be represented as a line "wound" on the torus (Fig. 3), and the Poincare section is a fractal (see, for example, (Schuster 1984)).

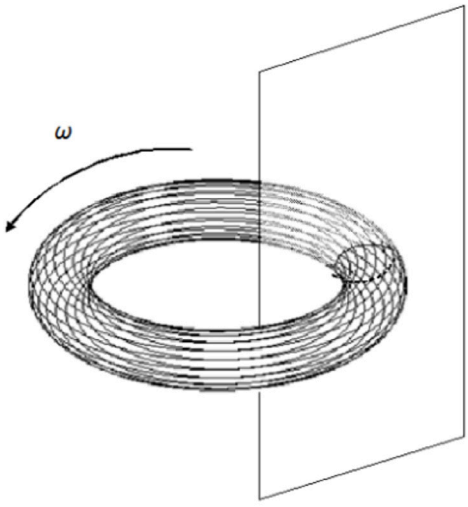

Fig. 3. Poincare cross section for the system (2)

 https://www.doi.org/10.33910/2687-153X-2021-2-3-122-131

The regularity of chaotic motion, which is clearly shown in the characteristic picture of the Poincare section allows us to introduce the probability density $\rho(\varphi,x,v)$, which determines the probability that the system is in the region of the phase space $d\varphi dxdv$ (Liapzev 2019; 2020):

$$dw = \rho\left(\varphi, x, \upsilon\right) d\varphi dx d\upsilon \,.$$

The probability density determined this way is normalized by one and satisfies the equation:

$$L\rho\left(\varphi, x, \upsilon\right) = 0\,, \tag{3}$$

where the differential operator L is defined by the expression:

$$L = \omega\frac{\partial}{\partial\varphi} + \frac{\partial}{\partial x} + \left(f\sin\varphi - \alpha x - \beta x^3 - \gamma\varphi\right)\frac{\partial}{\partial\upsilon}\,. \tag{4}$$

Equation (3), unlike the original Duffing equation (1), is a linear equation, so the probability density has properties characteristic of solutions of linear equations. In particular, for a small change in the operator L, the change in the probability density is also small. This allows us to use one or another version of the perturbation theory to calculate the average value of a certain physical quantity. That leads to the fact that if a change in the operator ΔL can be represented as a sum:

$$\Delta L = \sum \lambda_n \Delta L_n\,,$$

where λ_n are small parameters, then the average value of any physical quantity that depends on the variables φ, x, υ, is also a linear function of these parameters. A numerical experiment for the case of specific perturbation operators confirms the validity of the above statement (Liapzev 2020).

It should be noted that such linear properties occur only for chaotic motion, when the attractor is a chaotic attractor, and changes in the parameters keep the motion chaotic. The probability density in this case can be modeled as some smooth function of the variables φ, x, υ. In case of regular motion, the variables φ, x, υ are periodic functions of time, and the attractor is a limit cycle with a period $2\pi n/\omega$, where n is a natural number. Within a single period, the variables x and υ can be expressed as single-valued functions of the variable φ :

$$x = g\left(\varphi\right), \qquad \upsilon = h\left(\varphi\right)\,.$$

In accordance with equations (2), the functions $g(\varphi)$ and $h(\varphi)$ satisfy the equations:

$$\frac{dx}{d\varphi} = \upsilon\,,$$

$$\frac{d\upsilon}{d\varphi} = -\alpha x - \beta x^2 - \gamma\upsilon + f\sin\varphi\,.$$

The probability density in this case is no longer a smooth function, but can be expressed as the δ-functions:

$$\rho\left(\varphi, x, \upsilon\right) = C\delta(x - g(\varphi))\delta(\upsilon - h(\varphi))\,,$$

where C is the normalization coefficient. It is easy to show that the probability density determined in this way satisfies equation (3). However, small changes in the parameters of the equation in this case can lead to an abrupt change in the nature of the movement. As a result, with a small change in the parameters, the system may transfer to a new attractor in the form of a limit cycle or to a chaotic attractor.

Symmetry breaking for solutions of the Duffing equation

The potential corresponding to the conservative force in the Duffing equation is symmetric with respect to the coordinate inversion transformation. However, the equation of motion (1) itself does not have such a symmetry. Nevertheless, the symmetry is preserved if we use a set of transformations that leave equation (1) invariant:

$$x \to -x, \quad t \to t + 2\pi/\omega\,.$$

When moving from equation (1) to a system of autonomous equations (2), the set of transformations that leave this system invariant can be written as:

$$x \to -x, \quad v \to -v, \quad \varphi \to \varphi + \pi. \tag{5}$$

It is easy to see that the set of transformations (5) leaves the operator L, defined by equality (4), invariant. It follows from equation (3) that its solutions must be either even or odd functions with respect to the set of transformations (5). Since the probability density is by definition a positive value, we get the equation:

$$\rho(\varphi + \pi, -x, -v) = \rho(\varphi, x, v). \tag{6}$$

In the case of the W-potential, the probability density satisfies the relation (6) if the oscillations capture the regions of both minima. However, when the amplitude of the external field decreases, the oscillations are limited to either the region $x < 0$ or the region $x > 0$. This means that, depending on the initial conditions, one of the solutions exists: $\rho_<(\varphi, x, v)$, which turns to zero at $x > 0$, or $\rho_>(\varphi, x, v)$, which turns to zero at $x < 0$. The initial symmetry in this case manifests itself in the relations:

$$\rho_>(\varphi, x, v) = \rho_<(\varphi + \pi, -x, -v). \tag{7}$$

Let us now assume that for a certain set of parameters, the symmetry is broken, so that, depending on the initial conditions, the solutions $\rho_<(\varphi, x, v)$, or $\rho_>(\varphi, x, v)$, are realized, but the movements in both cases remain chaotic. Let us also assume that with some small change in the parameters, the symmetry is restored, and the character of the motion remains chaotic. This means that the symmetry breaking occurs when the operator L changes slightly. This, in turn, means that perturbation theory can be applied to find solutions. The case in question is similar to the quantum mechanical problem with W-potential. The solution for the probability density for chaotic oscillations involving both pits can be obtained from perturbation theory and in the zero order has the form:

$$\rho(\varphi, x, v) = \frac{1}{2}\left(\rho_<(\varphi, x, v) + \rho_<(\varphi + \pi, -x, -v)\right). \tag{8}$$

Thus, we can say that the principle of superposition of solutions is fulfilled, but, unlike the quantum mechanical problem, not for wave functions but for probability densities.

Numerical results

The validity of the above assumption can be verified by a numerical experiment. However, the attempt to use the solutions of the Duffing equations is unsuccessful. If, for some parameters, the oscillations are chaotic and capture the regions of both pits, that is, the transitions over the barrier realize, then when the symmetry is broken, the oscillation in the region of one of the pits turns out to be periodic, that is, instead of a chaotic attractor, the solution tends to the attractor in the form of a limit cycle. In this case, it is impossible to check the relation (8). The reason for the transition to the limit cycle is, apparently, that chaotic oscillations in the system described by the Duffing equation are realized either at large values of the amplitude of the driving force, or when there is a local maximum potential in the oscillation region. It is easy to show that for a quadratic potential, small oscillations, driving with harmonic force, can occur both in the case when the potential has a minimum (near the minimum) and in the case when the potential has a maximum (near the maximum). However, oscillations near the minimum are stable, and unstable near the maximum. Namely this kind of instability can generate chaotic motion.

The above considerations suggest that making the oscillations in the region of one of the pits chaotic when the symmetry is broken, it is necessary to complicate the shape of the potential by adding maxima to each of the pits. At the same time, it is desirable that for large values of the coordinate, the potential, like the potential in the Duffing equation, increases proportionally to the fourth power of the coordinate. In this paper, we used for the calculation the potential:

$$U(x) = x^4/4 + \alpha_0 Lor(x/\beta_0) + \alpha_1 Lor((x - dx)/\beta_1) + \alpha_1 Lor((x + dx)/\beta_1), \tag{9}$$

where the potential maxima are provided by the Lorentz distribution function:

$$Lor(x) = \frac{1}{1 + x^2}\ .$$

 https://www.doi.org/10.33910/2687-153X-2021-2-3-122-131

The parameters α_0 and α_1 determine the heights of the central and side local maxima, the parameters β_0 and β_1 determine the widths of these maxima, and the parameter dx determines the shift of the side maxima relative to the central maximum. For further calculations, the following values were used: $\alpha_0 = 7.5$, $\alpha_1 = 2.3$, $\beta_0 = \beta_1 = 0.3$, $dx = 1$. The potential graph is shown in Figure 4.

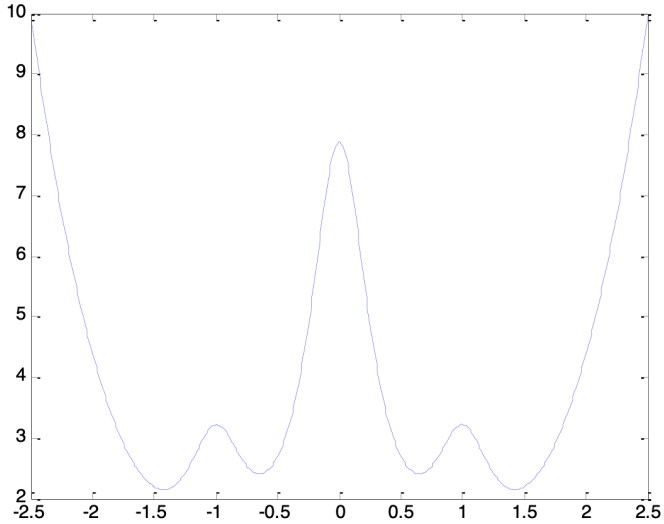

Fig. 4. Graph of the potential defined by the expression (9)

The numerical calculation was carried out for an equation similar to the Duffing equation, with a modified force:

$$\ddot{x} = F(x) - \gamma\dot{x} + f\sin\omega t\,,$$

where $F(x) = -\dfrac{\partial U}{\partial x}$ and $U(x)$ is defined by the expression (9). The parameters determining the dissipation and frequency of driving force were assumed to be equal, $\gamma = 0.2$, $\omega = 3.9$ respectively. The numerical calculation shows that at the value of the driving force amplitude $f = 1.85$, the oscillation at these parameter values is chaotic and captures the regions of both pits. Meanwhile, for quite long periods the oscillation occurs in one of the pits with rare jumps from one pit to another. For $f = 1.84$, a symmetry breaking occurs, so that the oscillation, which is also chaotic, is limited to the region of one of the pits, depending on the initial conditions.

The calculation of probability densities was carried out on a time interval equal to 10,000 periods of driving force. As a result of the calculation, a three-dimensional array $\rho(\varphi_i, x_j, v_k)$, was calculated. The array size is 120 × 101 × 101. The values of ϕ_i were distributed over the interval $[0,2\pi)$ in a regular way. The values of x_j and v_k were uniformly distributed over the intervals $[-x_{max}, x_{max}]$ and $[-v_{max}, v_{max}]$, respectively, where x_{max} and v_{max} are the maximum values of the coordinate and velocity modulus obtained as a result of calculations on this time interval.

Since the superposition principle is only statistically valid, an element-by-element comparison of the arrays included in equality (8) is meaningless. A visual comparison of the results can be illustrated by the graphs below.

The probability density averaged over the variable v

To graphically represent the probability density on a two-dimensional graph, we define the average density by the ratio:

$$\bar{\rho}(\varphi_i, x_j) = \frac{1}{N_v}\sum_{k=1}^{N_v}\rho(\varphi_i, x_j, v_k)\,,$$

where $N_v = 101$ is the dimension of the array along the v axis. Figure 5 shows graphs of the probability density $\bar{\rho}(\varphi_i, x_j)$ at $f = 1.84$, when the symmetry is broken, that is, oscillations occur in the region

of one of the pits depending on the initial conditions. On the horizontal axis, the x value is plotted, and on the vertical axis, the φ value is plotted. Darker areas correspond to a higher probability density.

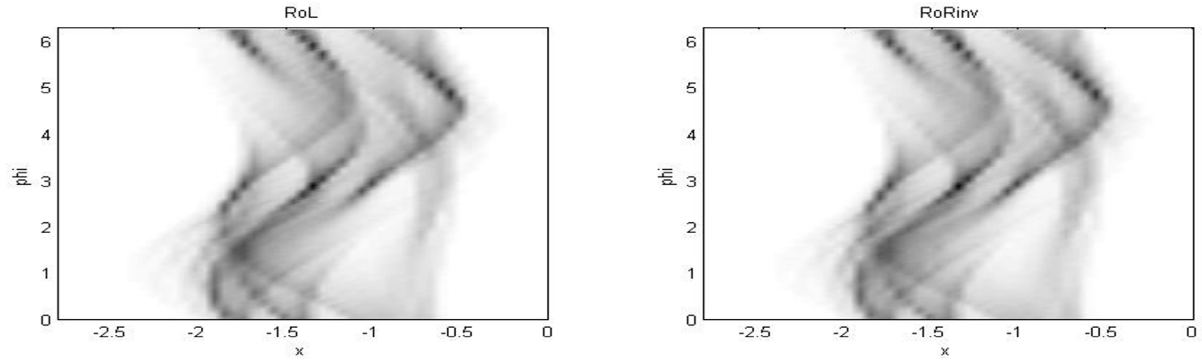

Fig. 5. Graphs of the average probability density (see the text)

The probability density distribution in the left graph corresponds to the oscillations in the left pit ($x < 0$). To clearly demonstrate the symmetry, the right graph shows the probability density of oscillations in the right pit ($x > 0$), transformed in accordance with the relations (5), that is, inverted with respect to x and shifted by π with respect to φ.

Figure 6 shows the probability density distribution graphs calculated at $f = 1.85$ (upper graph) and $f = 1.84$ (lower graph). To visually verify that the superposition principle is fulfilled, the probability density obtained for the left pit $\rho_{<}(\varphi, x, \upsilon)$, is shifted by π and inverted, after which the superposition (8) is calculated. Note that, due to the symmetry, an almost indistinguishable picture is obtained if instead of the relation (8) we use the relation:

$$\rho(\varphi, x,) = \frac{1}{2}\left(\rho_{<}(\varphi, x,) + \rho_{>}(\varphi, x,)\right).$$

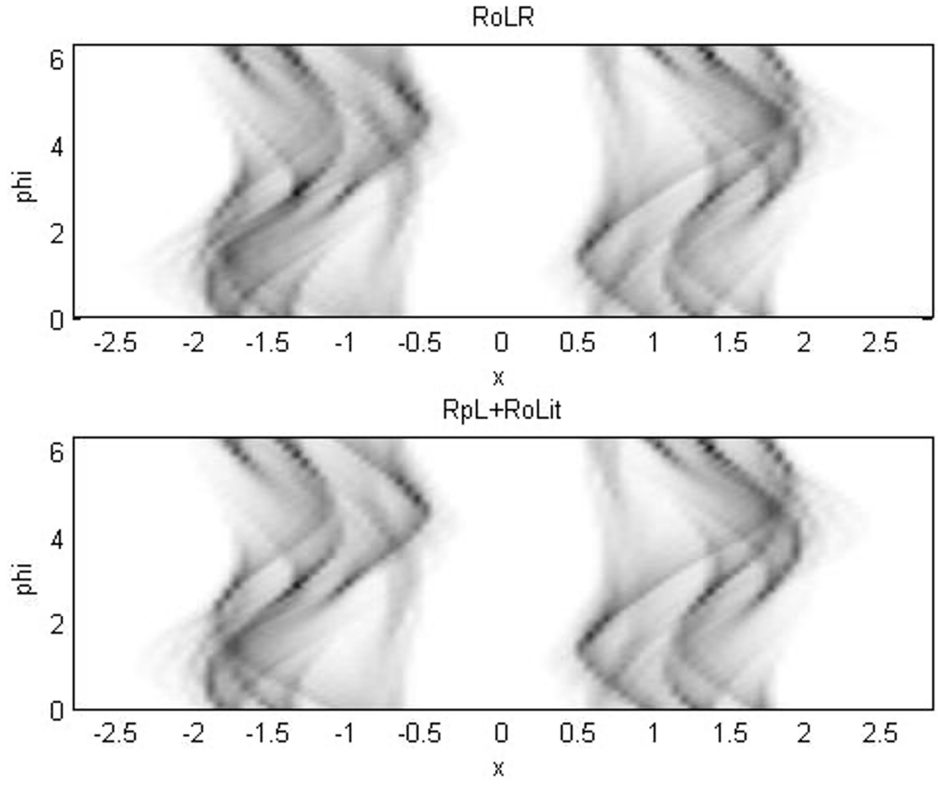

Fig. 6. Graphs of the average probability density (see the text)

 https://www.doi.org/10.33910/2687-153X-2021-2-3-122-131

Cross sections at ϕ = const

Other graphs that allow us to visually judge the fulfillment of relation (8) are the sections of the probability density graph at constant values of φ. Figure 7 shows the graphs at $\varphi = 0$ (left graphs) and $\varphi = \pi$ (right graphs).

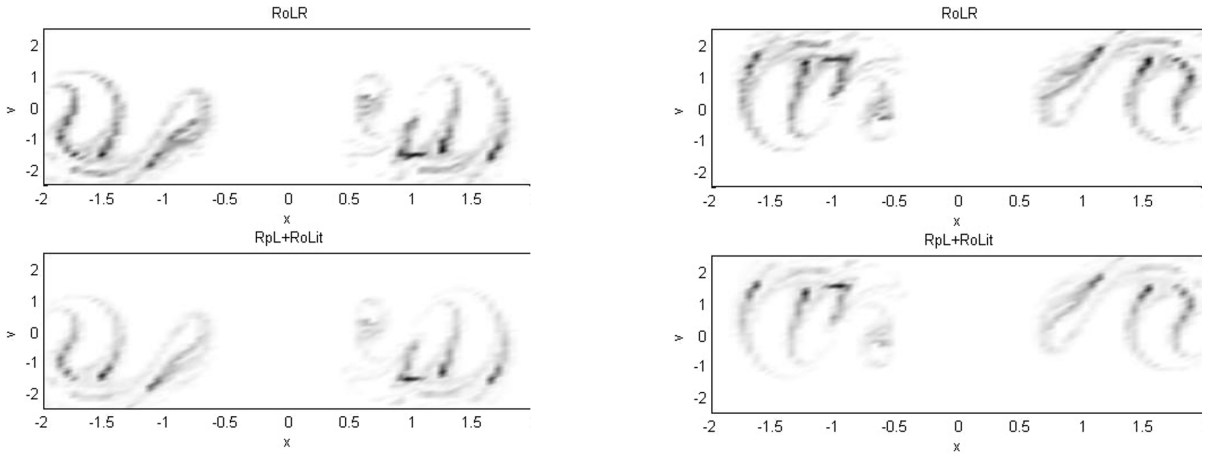

Fig. 7. Graphs of the probability density cross section (see the text)

As in the previous figures, the upper graphs correspond to the probability density calculated at $f = 1.85$, and the lower ones calculated at $f = 1.84$ for oscillations in the left pit and combined in accordance with the superposition principle (relation (8)). In addition to illustrating the superposition principle, the graphs also illustrate symmetry. Rotation of the right graphs by 180° around the axis perpendicular to the drawing plane (transformations $x \to -x$, $v \to -v$) gives an image that is almost indistinguishable from the left graphs.

Quantitative estimation of the results

To calculate a certain quantitative estimate of the fulfillment of the superposition principle, we turn to the equation for the probability density, which in the case of the potential chosen by us has the form:

$$\left(\omega\frac{\partial}{\partial\varphi}+\frac{\partial}{\partial x}+\left(f\sin\varphi-F\left(x\right)-\gamma v\right)\frac{\partial}{\partial v}\right)\rho\left(\varphi,x,v\right)=0\,, \tag{10}$$

where $F\left(x\right)=-\dfrac{\partial U}{\partial x}$, and $U(x)$ is defined by the expression (9). It is easy to show that if some positive function $\rho(\varphi, x, v)$, is found that satisfies equation (10), then for any real value p, the function $(\rho(\varphi, x, v))^p$, will also satisfy equation (10). Now, let us define the function:

$$\psi\left(\varphi,x,v\right)=\left(\rho\left(\varphi,x,v\right)\right)^{1/2}. \tag{11}$$

In the probabilistic sense, the function $\psi(\varphi, x, v)$ is analogous to the quantum mechanical wave function, its modulus square gives the probability density. However, first, the definition (11) does not allow us to uniquely define the function $\psi(\varphi, x, v)$, based on the function $\rho(\varphi, x, v)$. The function $\psi(\varphi, x, v)$ multiplied by an arbitrary phase factor depending on the variables φ, x, v, will also satisfy the relation $|\psi(\varphi, x, v)|^2 = \varrho(\varphi, x, v)$. Secondly, in this case, there are no properties similar to the properties of quantum mechanical wave function (quantization, interference, etc.). However, definition (11) can be used to quantify the proximity of two different solutions for the probability density. To do this, we can use the concept of a scalar product similar to the scalar product of quantum mechanical functions. For the two calculated probability densities $\rho_1(\varphi, x, v)$ and $\rho_2(\varphi, x, v)$, the scalar product of the corresponding functions $\psi_1(\varphi, x, v)$ and $\psi_2(\varphi, x, v)$ can be defined as follows:

$$\langle \psi_1 | \psi_2 \rangle = \frac{1}{N_\varphi N_x N_\upsilon} \sum_{i=1}^{N\varphi} \sum_{j=1}^{Nx} \sum_{k=1}^{N\upsilon} \psi_1 \left(\varphi_i, x_j, \upsilon_k \right) \psi_2 \left(\varphi_i, x_j, \upsilon_k \right), \quad (12)$$

where N_φ, N_x and N_υ determine the dimension of the array $\rho(\varphi_i, x_j, \upsilon_k)$. Obviously, the scalar product defined in this way can take a value from 0, when the probability densities are completely different, to 1, when the probability densities are completely the same. Thus, we can give the relations (7) and (8) some quantitative estimation. According to the relation (11), we define for the probability density $\rho_>(\varphi, x, \upsilon)$ the function $\psi_>(\varphi, x, \upsilon)$, and for the probability density $\rho_<(\varphi+\pi, -x, -\upsilon)$, the function $\psi_{<it}(\varphi, x, \upsilon)$. Calculated in accordance with the above definition, the scalar product gives the following value: $\langle \psi_> | \psi_{<it} \rangle \approx 0.98$. This quantitatively confirms the manifestation of the properties of symmetry presented in the above figures.

Similarly, to quantify the validity of the principle of superposition of solutions (8), we define for the probability density $\rho(\varphi, x, \upsilon)$ function $\psi(\varphi, x, \upsilon)$ according to the relation (11), and for the probability density $\frac{1}{2}\left(\rho_<(\varphi, x, \upsilon) + \rho_<(\varphi+\pi, -x, -\upsilon)\right)$ (the right part of equality (8)), the function $\psi_{superp}(\varphi, x, \upsilon)$. Then the numerical evaluation of the validity of the superposition principle can be determined by calculating the scalar product of the functions $\psi(\varphi, x, \upsilon)$ and $\psi_{superp}(\varphi, x, \upsilon)$ in accordance with the definition of the scalar product (12). The result of the calculations $\langle \psi | \psi_{superp} \rangle \approx 0.95$ corresponds to the similarity of the graphs shown in Figures 6 and 7.

The superposition principle in classical systems with dynamic chaos and in quantum mechanical systems

From the above, an analogy follows between the quantum mechanical problem, in which the symmetry breaking is considered, and the problem of classical dynamics, which admits a solution with dynamic chaos. Just as in a quantum mechanical problem, the use of the superposition principle (Feynman et al. 2006) can be justified by applying perturbation theory to the linear equation that determines the solution of the problem. Indeed, let equation (10), which can be written as:

$$L\rho(\varphi, x, \upsilon) = 0,$$

where

$$L = \omega \frac{\partial}{\partial \varphi} + \frac{\partial}{\partial x} + \left(f \sin\varphi - F(x) - \gamma \upsilon \right) \frac{\partial}{\partial \upsilon},$$

define the probability density of chaotic motion and have two solutions $\rho_<(\varphi, x, \upsilon)$ and $\rho_>(\varphi, x, \upsilon)$, which correspond to chaotic motion in the region of the left ($x < 0$) and right ($x > 0$) pits of a potential similar to W-potential (9). Due to the symmetry of the problem, the relation (7) holds. We will consider the operator L as an unperturbed operator. Let a small addition (perturbation):

$$V = \Delta f \sin\varphi \frac{\partial}{\partial \upsilon} \quad (13)$$

to the unperturbed operator lead to the fact that the solution of the equation

$$(L + V)\rho(\varphi, x, \upsilon) = 0$$

describes the chaotic movement that captures both pits. The solution $\rho(\varphi, x, \upsilon)$ in this case can be obtained by perturbation theory. In the zero approximation for $\rho(\varphi, x, \upsilon)$, we get the former equation. However, since the solution must now describe the motion in both pits, it is necessary to take a superposition of the solutions $\rho_<(\varphi, x, \upsilon)$ and $\rho_>(\varphi, x, \upsilon)$. The symmetry properties and positivity of the $\rho(\varphi, x, \upsilon)$ function allow us to obtain only the solution proportional to the sum of the solutions $\rho_<(\varphi, x, \upsilon)$ and $\rho_>(\varphi, x, \upsilon)$, and from the normalization condition it follows that the coefficient for the sum must be equal to 1/2.

The numerical experiment confirms the above relations. We have given just one concrete example. Calculations show that with an increase in the perturbation operator (13), that is, with an increase in the value of Δf, the corrections of the 1st order of the perturbation theory increase. This manifests itself in a decrease in the value of $\langle \psi_> | \psi_{<it} \rangle$.

The introduction of functions proportional to the root of the probability density is convenient for evaluating the accuracy of perturbation theory calculations. However, they cannot be given the same

 https://www.doi.org/10.33910/2687-153X-2021-2-3-122-131

meaning of wave functions as in a quantum mechanical problem. This statement can be illustrated by the following example. As mentioned above, in a quantum mechanical problem with *W*-potential, the probability of detecting a molecule in the region of one of the local minima oscillates according to the law expressed by:

$$w = (\sin \Delta Et / \hbar)^2 . \tag{14}$$

These oscillations are manifested in the spectra of the corresponding systems. In the classic problem under consideration, we also observe jumps from one pit to another with long intervals of chaotic motion in the region of each of the pits. However, the numerical experiment shows that there is no regular periodicity similar to the oscillations (14). This statement is confirmed by the fact that the calculated Fourier spectrum for such motions does not have any clearly expressed maximum, in addition to the maximum at the frequency of the driving force ω.

Conclusion

This paper investigated only one special case of chaotic motion in the problem of classical nonlinear dynamics, however, the obtained conclusions can be generalized to other systems where dynamic chaos manifests itself. These conclusions can be formulated as follows.

1) Chaotic motion in dissipative systems of classical dynamics can be characterized by the probability density of states in the phase space. The function corresponding to the probability density can be obtained by solving a partial differential equation.
2) For the solutions of this classic problem, the principle of superposition of solutions is valid, as is the case with the quantum mechanical problem.
3) The validity of the superposition principle can be most effectively shown in the problem that admits a symmetry breaking when changing some parameters. The validity is confirmed by the numerical experiment.

Conflict of interest

Author declares that there is no conflict of interest.

References

Bunker, P. R. (1979) *Molecular symmetry and spectroscopy*. New York: Academic Press, 440 p. (In English)

Feynman, R. P., Leighton, R. B., Sands, M. (2006) *The Feynman lectures on physics including Feynman's tips on physics: The definitive and extended edition. Vol. 2.* 2nd ed. Boston: Addison-Wesley Publ., 512 p. (In English)

Landau, L. D., Lifshitz, E. M. (1977) *Quantum mechanics: Non-relativistic theory. Vol. 3.* 3rd ed., rev. Oxford et al.: Pergamon Press, 688 p. (In English)

Liaptsev, A. V. (2013) Simmetriya regulyarnykh i khaoticheskikh dvizhenij v zadachakh nelinejnoj dinamiki. Uravnenie Duffinga [The symmetry of regular and chaotic motions in nonlinear dynamic problems. Duffing equation]. *Izvestia Rossijskogo gosudarstvennogo pedagogicheskogo universiteta im. A. I. Gertsena — Izvestia: Herzen University Journal of Humanities & Sciences*, 157, 24–34. (In Russian)

Liapzev, A. V. (2019) The calculation of the probability density in phase space of a chaotic system on the example of rotator in the harmonic field. *Computer Assisted Mathematics*, 1, 55–65. (In English)

Liapzev, A. V. (2020) Linear properties of chaotic states of systems described by equations of nonlinear dynamics. Analogy with quantum theory. *Physics of Complex Systems*, 1 (4), 150–157. https://doi.org/10.33910/2687-153X-2020-1-4-150-157 (In English)

Schuster, G. H. (1986) *Deterministic chaos. An introduction.* Weinheim: Physik-Verlag, 220 p. (In English)